

An Experimental Study on Appearance of Flow in Multisection MR Imaging of Laminar Flow

Jae Hyung Park, M.D., Tae Hwan Lim, M.D.,* Hyung Jin Kim, M.D., Man Chung Han, M.D.,
Chu-Wan Kim, M.D., Chi Woong Moon, M.D.,** Zang Hee Cho, Ph.D.**

Department of Radiology, College of Medicine, Seoul National University

**Present Address : Research Fellow in Magnetic Resonance Imaging,*

Department of Radiology, University of California, San Francisco

***Department of Electric Science, Korea Advanced Institute of Science*

층류의 다절편 자기공명영상에서의 유체현상에 대한 실험적 연구

서울대학교 의과대학 방사선과학교실 및 한국과학기술원 전기전자공학과*

박재형 · 임태환 · 김형진 · 한만청 · 김주완 · 문치웅* · 조장희*

□ 국문초록 □

다절편 자기공명에서 유체현상의 양상을 관찰하기 위하여 2.0 Tesla 자기공명영상기를 이용한 유체모형 실험을 시도하였다.

제1절편에서의 유체영상은 와류형성속도에 이르기까지 모든 유속에서 균질성으로 나타났다. 제2절편 영상은 그와는 달리 균질성 음영에서 환형, 표적형, 그리고 작은 원형으로 변화하였고 와류형성속도 이상인 경우 영상이 왜곡되어 불규칙하여졌으며 한계속도(cut-off velocity)에 도달한 후에는 영상신호가 완전히 소실되었다. 유속이 느릴때의 균질성 음영은 완전히 자화된 스핀들이 반복시간(repetition time)동안 유입됨에 따른 결과이며 제2절편에서는 더 높은 유속에서 부분자화된 스핀의 유입과 완전자화 스핀이 절편이동시간(section transit time)동안 유입된 효과가 추가되어 환형, 표적형 및 작은 원형을 초래하는 것으로 설명된다.

= Abstract =

In order to observe the pattern of a flow image on multisection MR imaging technique, a flow phantom experiment was performed using a superconducting high field 2.0 Tesla MRI scanner.

The pattern of the first section images was homogeneous round at all flow velocities until the turbulence forming level. The patterns of the second section images, however, changed into a homogeneous round shape, a ring shape, a target shape, and a small round shape as the velocity increased. When scanned at velocities higher than the turbulence forming level, the images become distorted and irregular, and eventually disappeared after the cut-off velocity.

The homogeneous round image seen at the lower velocity levels is thought to be due to the overwhelming effects of fully magnetized spins influxed into the imaging section during the prior repetition time (TR). Later in the high velocity levels the effects of the partially saturated spins and fully magnetized spins influxed during the section transit time (TR/slice number) are added, and result in ring, target, and small round patterns in the second section image.

KEY WORDS : Magnetic resonance, experimental • Blood vessels, MR studies • Blood, flow dynamics.

INTRODUCTION

In MR imaging, it is well known that rapid flow shows signal loss that induces the natural contrast of blood flow in the cardiovascular system with neighboring anatomical structures¹⁻⁶. In addition to the high velocity signal loss, other flow phenomena such as flow related enhancement, even-echo rephasing and pseudogating were also reported⁷⁻⁹.

In multisection imaging of flow, paradoxical enhancement can be seen at the slow flow velocity levels in the entry slice⁷, and the pattern of the transaxial flow image is known to change with regards to the flow velocity in each slice of multisection MR imaging^{8,10}.

We performed an experimental phantom study to see the changes in patterns of MR flow images in transaxial multisection MR imaging especially at the first and the second slices. Theoretical interpretations for the various image patterns were attempted.

MATERIALS AND METHODS

1. Flow phantom

Three parallel soft PVC tubes, with 0.96cm inner diameter each, were used as the flow phantom. Each tube has its own flow adjuster connected to a water tank. The central tube was filled with stationary water in order to get the control image. The length of the straight portion of each tube was

2.0cm ; long enough to eliminate the chance of turbulence formation due to the curvature of the tube. Plain tap water ($T_1 = 1536\text{msec}$, $T_2 = 297\text{msec}$) was used as the flowing material. The flow velocities were adjusted to get nine different levels from 0.5 cm/sec through 42.3cm/sec.

2. MR Imaging

A superconducting 2.0 Tesla MRI scanner developed by the Korea Advanced Institute of Science was used. The applied field gradient was 0.2G/cm and the matrix number was 256×256 . All the images were obtained from the two dimensional Fourier Transformation method. All the scans were performed using a spin-echo technique in which a 90° excitation pulse was followed by a 180° refocusing pulse. The applied TR was 400msec and 800msec and the TE was 27msec. Transaxial multisection images of 5 slices were taken with 1cm of slice thickness at 9 different velocity levels.

3. Image analysis

The signal intensity was obtained from the circular region of interest (ROI) in each transaxial flow image at the first slice of the multisection images. The ROI was composed of 8 or 14 pixels according to the size of the images. The signal intensity (I) of each flow image was compared with that of the stationary water (I_0).

The changes of the image patterns in relation to the flow velocity were analysed in the first and the second section with a particular interest on the characteristics of laminar flow.

RESULTS

The first slice

The transaxial MR imaging of the flow phantom showed a homogeneous round pattern throughout all velocity levels until turbulence formation (Fig. 1). As the velocity increased above the level of turbulence formation, the image became distorted

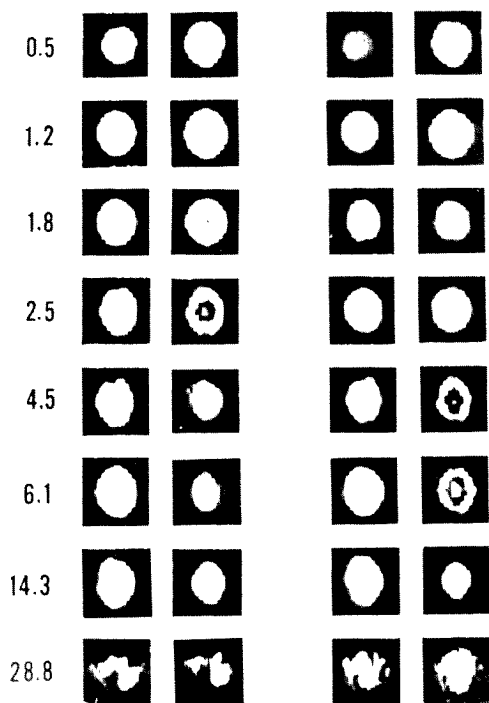


Fig. 1. Changes of flow appearance in relation to the flow velocity, TR, and location of imaging section in multisection imaging technique. First section images show homogeneous round pattern at velocity range of 0.5cm/sec-14.3cm/sec in both TRs. Second section images show more variable patterns by different velocity levels and TRs : homogeneous round, ring shape, target shape, and small round images. Images are distorted and irregular at velocity 28.8cm/sec due to turbulence formation regardless of TR and location of imaging section. TR : Repetition time. TE : Echo time. 1st : First section image. 2nd : Second section image.

and irregular, and eventually was lost.

Relative signal intensity (I/I_0) increased as the velocity increased at slow velocity levels. The maximum value of I/I_0 was 2.39, and it was given at the flow velocity 1.85cm/sec (V_{max}), when scanned with TR 800msec. When scanned with TR 400msec, the maximum value of I/I_0 and the V_{max} was 3.42 and 2.5cm/sec respectively. After reaching a peak, the signal intensity decreases as the velocity increased (Fig. 2).

The second slice

With TR 800msec, the image pattern was homogeneous round at slow velocity levels (0.5cm/sec and 1.2cm/sec) as seen in the first section image. As the velocity increased the image pattern showed variable shapes : a thick ring shape at 1.8cm/sec, a thin ring shape with a faint central intensity at 2.5cm/sec, and small round shape at the high velocity levels (4.5cm/sec, 6.3cm/sec, and 4.3cm/sec). At the velocity 28.8cm/sec, the image became distorted and irregular just as seen in the first section image. No signal was seen at the velocity 42.3cm/sec (Fig. 1).

With TR 400msec, homogeneous round shape was seen at slow velocity levels through 2.5cm/sec. The image pattern changed as the velocity increased : a thin ring shape with a faint central intensity at 4.5 cm/sec, a target shape at 6.3cm/sec, and a small round shape at 14.3cm/sec. At the velocity above the turbulence forming level, the images become distorted and finally disappeared as in the scans with TR 800msec (Fig. 1).

DISCUSSION

The signal intensity of the first section image was influenced by the influx of fully magnetized spins into the imaging section during the repetition time and wash-out of excited spins from the imaging section during the time between 90° pulse and 180° pulse.

In the plug flow model, the position of a spin along

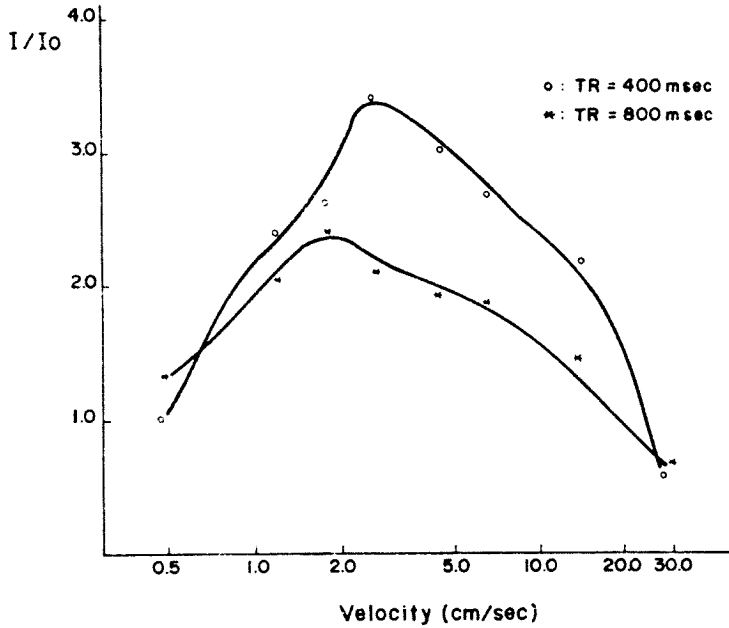


Fig. 2. Change of signal intensity with regards to the flow velocity and TR. Relative intensity(I/I_0) is initially increased as velocity increase. After reaching peak, intensity decreases as velocity continues to increase. Enhancement of signal intensity is more accentuated with scanned with short TR. I : Intensity of flowing water. I_0 : Intensity of the stationary water. TR : Repetition time.

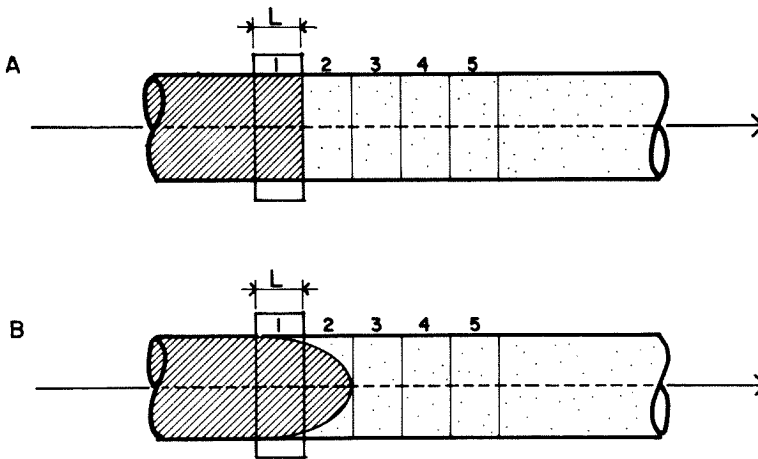


Fig. 3. Difference of profile between plug flow and laminar flow explaining inflow signal enhancement. A : Plug flow. Effect of inflow enhancement at first section becomes maximum when velocity is L/TR . B : Laminar flow. Amount of influxed fully magnetized spin at first section is less than that seen in plug flow, because spins at central portion of laminar flow start to leave imaging section when mean velocity becomes higher than $L/2TR$. L : Slice thickness. 1-5 : Slice number in multisection imaging. : Fully magnetized spins. : Partially saturated spins.

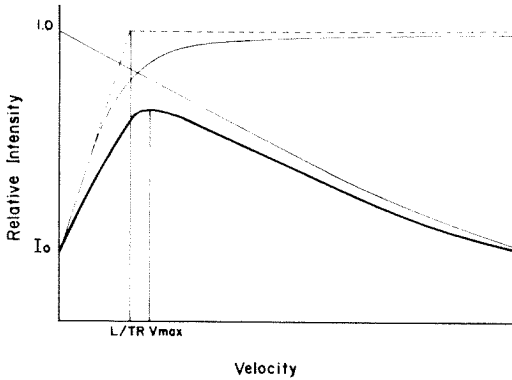


Fig. 4. Comparison of the effect of inflow signal enhancement between plug flow and laminar flow. In Plug flow, effect of inflow signal enhancement increases linearly as velocity increases until reaching peak at velocity $V=L/TR$. In laminar flow, the effect increases linearly as velocity increases until mean velocity reaches $L/2TR$. After that velocity, it converges to the maximum value. I_0 : Intensity of stationary water. L : Slice thickness. TR : Repetition time.

— : Change in plug flow.
 — : Change in laminar flow.

the axis of the flow, X , is represented as a equation

$$X = V \cdot T, \dots\dots\dots (1)$$

When V is the velocity of flow and T is the time lapsed. According to the equation(1), the influx of fully magnetized spins into the imaging section reaches the maximum value when V is L/TR (L : slice thickness, TR : repetition time).

In the laminar flow model, as the velocity phase shows the parabolic pattern(Fig. 3), the position of a spin along the axis of the flow, X , can be represented as a equation

$$X = \frac{2\bar{V}}{R^2} \cdot (R^2 - Y^2) \cdot T, \dots\dots\dots (2)$$

When \bar{V} is the mean velocity, R is the half radius of the conduit, Y is the distance from the central axis of flow along the perpendicular direction, and T is the time lapsed¹¹.

According to the equation²¹, the amount of the fully magnetized spins influxed into the imaging section

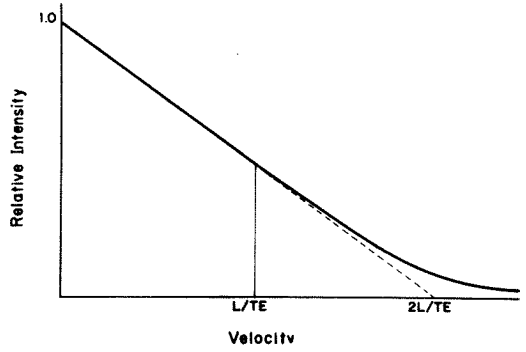


Fig. 5. Comparison of the effect of outflow signal loss between plug flow and laminar flow. In plug flow, signal intensity decreases linearly from maximum value "1.0" (at $V=0$) to "0" (at $V=2L/TE$). In laminar flow, signal intensity decreases linearly as seen in plug flow until mean velocity reaches L/TE . Thereafter it converges to "0". L : Slice thickness. TE : Echo time.

— : Change in plug flow.
 — : Change in laminar flow.

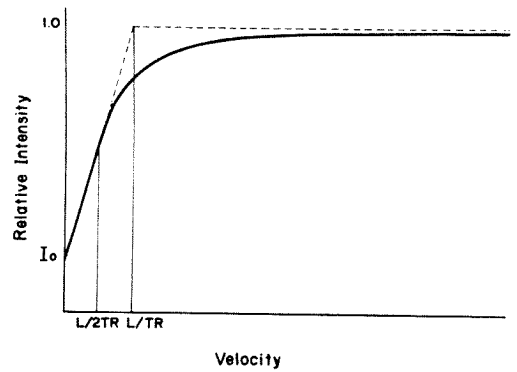


Fig. 6. Sum of the effects of inflow signal enhancement and outflow signal loss. Note the fact that small TR gives small I_0 value and, in turn, small I_0 gives large I/I_0 value; and that V_{max} takes larger value in laminar flow than in plug flow. I_0 : Intensity of stationary water. TR : Repetition time. V_{max} : Velocity that gives maximum intensity. L : Slice thickness.

— : Change in plug flow.
 — : Change in laminar flow.
 — : Sum of the effects in laminar flow.

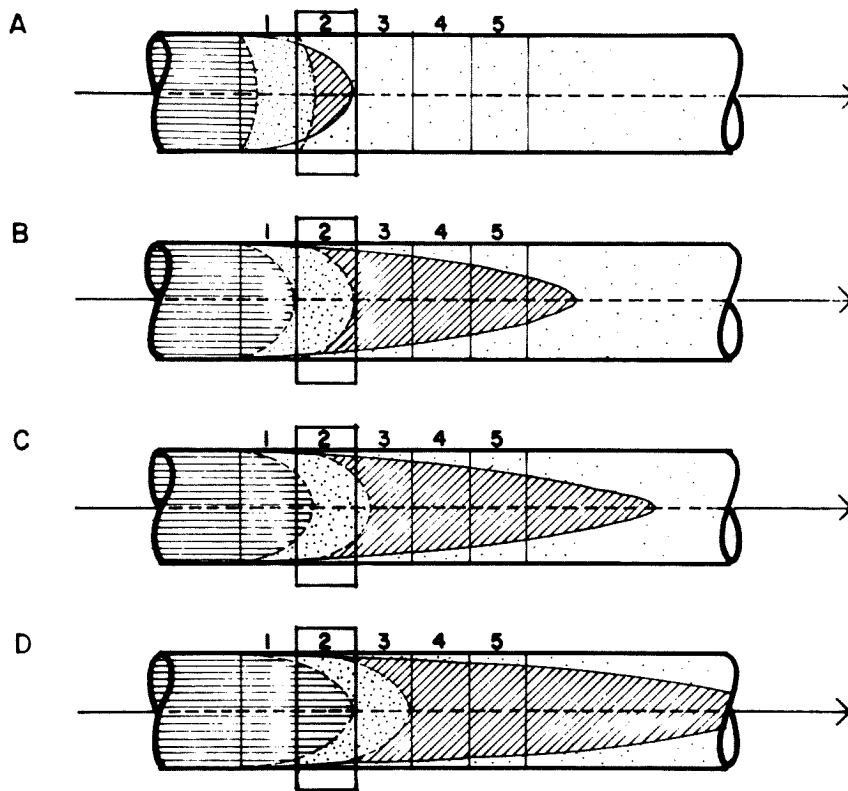


Fig. 7. Diagrams explaining the diversity of flow profile in the second section image with regards to flow velocity. A : Dominant effect of fully magnetized spins influxed primarily during prior TR results in homogeneous round image. B : Combined effect of fully magnetized spins influxed primarily during prior TR and partially saturated spins influxed from the first section during section transit time ($TR/\text{number of slices} ; TT$) result in ring shape image. C : Additional effect of fully magnetized spins influxed secondarily during TT results in target shape image. D : Dominant effect of fully magnetized spins influxed secondarily during TT results in small round image.

-  : Fully magnetized spins influxed primarily during prior TR.
-  : Spins that experienced RF pulse at the first section.
-  : Fully magnetized spins influxed secondarily during TT.
-  : Spins that experienced RF pulse during prior TR.

during the time TR increases linearly as a function of time until the velocity reaches $L/2TR$, and after then, it converges to the maximum value (Fig. 4). The wash-out of the excited spins during the time $TE/2$ shows the same pattern ; a linear relation until the velocity of L/TE , and a convergence to the maximum value after then (Fig. 5). Figure 6 shows the sum of the effects of flow relates signal

enhancement and the high velocity signal loss in the laminar flow model represented by the intensity curve as a function of time. The intensity curve shows the fact that a small TR value gives a small I_0 value, and in turn, a large I/I_0 value ; and that the V_{max} takes a larger value in the laminar flow than in the plug flow.

In the first section imaging, although a decrease

in the size of the image due to the peripheral signal loss according to the dephasing effect of spins could be expected at high velocity levels¹²⁾¹³⁾, no significant changes in the size of the image were appreciated in this experiment. In the second section imaging, however, the size of the image become smaller at high velocity levels. From these facts, it is suggested that the time of flight effect plays a more important role in the construction of the image pattern than the odd echo dephasing effect does.

In the second slice, the flow image is influenced not only by the fully magnetized spins influxed into the imaging section during TR, which is the main factor for the homogeneous round shape of the first and second section images at the slow velocity levels(Fig. 7-A), but also by some other additional factors. As the first additional factor, we can think about the influx of the partially saturated spins, received RF pulse at the first slice, into the imaging section during section transit time. This effect results in loss of signal intensity in the central portion of the transaxial image, and hence comes the ring shaped image(Fig. 7-B). At the higher velocity level, there occurs a secondary influx of fully magnetized spins during the section transit time.

The combined effects of fully magnetized spins influxed primarily during TR, partially saturated spins influxed during the section transit time, and fully magnetized spins influxed secondarily during the section transit time form the target shaped image(Fig. 7-C). As the velocity increases more, the portion of the imaging section replaced by the fully magnetized spins influxed secondarily during the section transit time becomes greater, and consequently the image shows a homogeneous round pattern again, however, with a smaller size than the round image seen at the slow velocity levels (Fig. 7-D).

In this experiment the turbulence of flow was expected at the velocity higher than 21.9cm/sec (Reynolds number > 2100)¹⁴⁾. The distorted and irregular images obtained at the velocities above that level are thought to be the result of turbulence formation.

The understanding of the characteristics of laminar flow and variable flow image patterns seen on the multisection MR imaging technique will be helpful to the correct interpretation of clinical MR images and further experimental works as well.

References

- 1) Higgins CB, Byrd BF, Farmer DW, Osaki L, Silverman NH, Cheitlin MD : *Magnetic resonance imaging in patients with congenital heart disease. Circulation* 1984 ; 70 : 851-860
- 2) Higgins CB, Byrd BF, McNamara MT, Lanzer P, Lipton MJ, Botvinick EH, Schiller NB : *Magnetic resonance imaging of the heart ; a review of the experience in 172 subjects. Radiology* 1985 ; 155 : 671-679
- 3) Higgins CB, Byrd BF, Stark D : *Magnetic resonance imaging of hypertrophic cardiomyopathy. Am J Cardiol* 1985 ; 55 : 1121-1125
- 4) Higgins CB, Lanzer P, Stark D, et al : *Imaging by nuclear magnetic resonance in patients with chronic ischemic heart disease. Circulation* 1984 ; 69 : 523-531
- 5) Fletcher BD, Jacostein MD, Nelson AD, Riemenschneider TA, Alfidi RJ : *Gated magnetic resonance imaging of congenital cardiac malformations. Radiology* 1984 ; 150 : 137-140
- 6) Von Schulthess GK, Fisher M, Crooks L, Higgins CB : *Gated MR imaging of the heart ; Intracardiac signals in patients and healthy subjects. Radiology* 1985 ; 156 : 125-132
- 7) Crooks LE, Mills CE, Davis PL, et al : *Visualization of cerebral and vascular abnormalities by NMR imaging, the effect of imaging parameters on contrast. Radiology* 1982 ; 144 : 843-852
- 8) Herfkens RJ, Higgins CB, Hricak H, et al : *Nuclear magnetic imaging of atherosclerotic disease. Radiology* 1983 ; 148 : 161-166
- 9) Bradley WG, Waluch V : *Blood flow ; magnetic resonance imaging. Radiology* 1985 ; 154 : 443-450
- 10) Herfkens RJ, Higgins CB, Hricak, et al : *Nuc-*

- lear magnetic resonance imaging of the cardiovascular system ; normal and pathologic findings. Radiology 1983 ; 147 : 749-759*
- 11) Schlichting H : *Boundary layer theory. 6th ed. New York : McGraw-Hill, 1968 ; 78-80*
 - 12) Valk PE, Hale JD, Crooks LE, Vaufrman L, Roos MS, Ortendahl DA, Higgins CB : *MRI of blood flow ; Correlation of image appearance with spin-echo phase shift and signal intensity. AJR 1986 ; 146 : 931-939*
 - 13) Bradley WG, Waluch V, Lai K, Fernandez EJ, Spalter C : *The appearance of rapidly flowing blood on magnetic resonance images. AJR 1984 ; 143 : 1167-1174*
 - 14) Bird RB, Stewart WE, Lightfoot EN : *Transport phenomena. New York. Wiley, 1960 ; 153-158*